

Short communication

Synthesis of novel benzothiazole based fluorescent and redox-active organic nanoparticles for their application as selective and sensitive recognition of Fe³⁺ ions

Navneet Kaur^{*}, Randeep Kaur, Ranjeet Kaur, Shweta Rana^{*}

Panjab University, Chandigarh, Punjab, India



ARTICLE INFO

Keywords:

Benzothiazole
Organic nanoparticles (ONPs)
Fluorescence sensing
Electrochemical sensing

ABSTRACT

A novel benzothiazole based compound (**1**) has been synthesized and further employed for the fabrication of fluorescent as well as redox active organic nanoparticles (**1-ONPs**) by adopting a nano-re-precipitation method. The formation of **1-ONPs** was confirmed by Dynamic Light Scattering (DLS) and Transmission Electron Microscopy (TEM) techniques, where the size was found to be ~42.84 nm in the optimized conditions. The resulting **1-ONPs** acted as selective and sensitive sensor for recognition of Fe³⁺ ions in dual transduction mode. The nanoparticles underwent quenching of fluorescence intensity as well as an amplified stripping current response in the presence of Fe³⁺. The high surface charge density worked as a tool for enhancing the current response of nanoparticles over bulk solution mode and hence is extended to in-field analysis.

1. Introduction

Introduction of nano materials to the scientific word has unveiled large number of possibilities for engineering different types of materials of great interest [1]. The exceptional combination of small size and prominent properties of nano-materials is continuously carving their path towards their involvement in every type of research area such as medicine [2], analytical [3], electronics [4], chemosensors [5] etc. Along with the outstanding advantages of nano-materials, there are some biological issues related to their biodegradability. Inorganic nano-materials possess very high stability due to which they are very difficult to decompose. Along with this, they are highly penetrating in living bodies [6]. On the other hand, the stability of organic nano particles (ONPs) is dependent on various factors due to which their working environment is very limited. Due to this nature, ONPs are unlikely to persist in solution with unoptimized physical parameters such as temperature, pH and solvent system that tend to agglomerate in unfriendly conditions [7]. Therefore, ONPs do not pose major threat to the living bodies unlike inorganic nanoparticles. Evidences of ONPs employed for sensing purpose can be found in literature [8,9]. Kaur et al. [10] explored rhodamine based ONPs for sensing of Al³⁺ and adenosine monophosphate. The sensor showed fluorescence enhancement in the presence of Al³⁺ ion through spiroactam ring opening process. Mahajan

et al. [11] have also designed fluorescent organic nanoparticles based chemosensors using rhodamine derivative. The chemosensor experienced fluorescent enhancement on chelation with Hg²⁺ ions stated as chelation enhanced fluorescence (CHEF).

In sensing, electroanalytical methods pose advantages of ease of operation, portability, simple instrumentation and sample preparation. However, very limited research work has been reported by authors utilizing the electrochemical properties of ONPs for metal ion sensing. Billing et al. [12] have developed electrochemical sensor for PO₄³⁻ ions utilizing ONPs derived from Schiff's base receptor. The method offered good detection limit ranged in nM and was exploited to determine the amount of phosphate in biologically important samples. Recently, Kumar et al. [13] utilized ONPs of Schiff base for voltammetric detection Cu(II) ions. However, to the best of our knowledge till date, stripping voltammetric approach [14,15] has not been utilized for the metal ions sensing via ONPs, which is assumed to be better in terms of sensitivity and selectivity for the detection of metal ions [16] in comparison to other voltammetric techniques.

Among the various metal ions present in the biological systems, Fe³⁺ ion dictates its importance by catalysing various biological reactions that are fundamental to life of a living specie. One of the examples is haemoglobin, the organometallic protein of high importance, requires iron for performing its function of oxygen transport to all body parts.

^{*} Corresponding authors.

E-mail addresses: neet_chem@pu.ac.in (N. Kaur), shweta0402@pu.ac.in (S. Rana).

<https://doi.org/10.1016/j.inoche.2021.108648>

Received 14 March 2021; Received in revised form 22 April 2021; Accepted 29 April 2021

Available online 4 May 2021

1387-7003/© 2021 Elsevier B.V. All rights reserved.

The low iron content in the body leads to various problems like including anaemia and decrease in cognitive abilities. Whereas the excessive presence of Fe in the body can give birth to health issues like hereditary hemochromatosis. Iron is taken by our body through various types of iron rich foods for which the ultimate source of iron is the environment [17]. Therefore, to keep a check on the presence of iron in the water samples around us, sensing of iron is necessary. Dong et.al. had synthesized benzimidazole functionalized Zr-UiO-66 nanocrystals for sensing of Fe³⁺ ion that work efficiently in aqueous system [18]. For fast and highly sensitive detection of Fe³⁺ ion, Xu et al. had synthesized a two-dimensional metal organic framework nanosheets. The high surface area of nano-porous sheets was responsible for high sensitivity of the sensor [19]. Keeping this in mind, here organic nanoparticles based sensor has been designed using a dual mode response mechanism of optical and redox behaviour for the very first time to sense Fe³⁺. The tailoring methodology offered here facilitates the formation of ONPs due to increase in the possibility of π - π interactions between the molecules in solution phase [20].

2. Experimental

2.1. Materials and instrumentation

The detailed information about materials used for synthesis of compound **1**, its nanoparticles **1-ONPs**, evaluation of its optical studies along with quantum yield determination as well as redox studies and instruments used for its structural elucidation has been given in SI.

2.2. Synthesis of benzene-1,3-bis(benzothiazole) (**1**) and its organic nanoparticles **1-ONP**

Compound **1** has been synthesized by reaction of 2-aminothiophenol and benzene-1,3-dicarbaldehyde using microwave conditions (Scheme 1). The simple and cost-effective re-precipitation method was used to prepare an aqueous suspension of ONPs of compound **1** (**1-ONPs**). The detailed synthesis has been given in SI.

2.3. General procedure of fluorescence and electrochemical measurements for metal ion recognition using **1-ONPs**

The details for the general procedure of fluorescence and electrochemical measurements for metal ion recognition of **1-ONPs** has been given in SI.

3. Results and discussion

3.1. Fabrication of organic nanoparticles (**1-ONPs**) of compound **1**

For real time applications of sensors in environmental and biological domains, aqueous medium plays an important role. Since organic

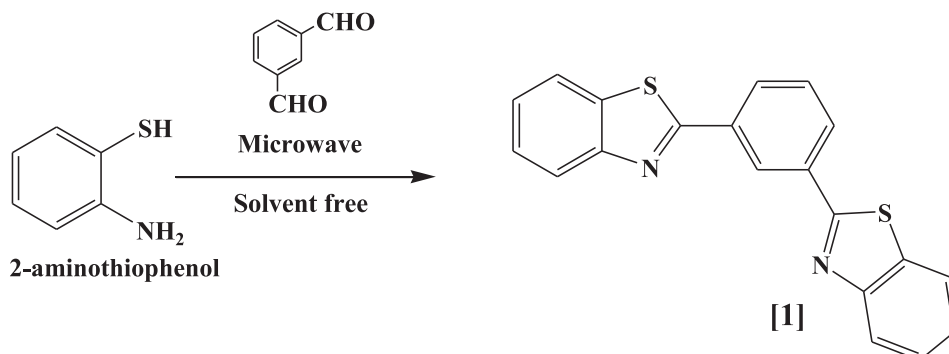
compound **1** had poor solubility in water, so their organic nanoparticles have been fabricated in DMSO:H₂O (1:99, v/v) solvent system. The re-precipitation method, being advantageous in terms of being extremely efficient, less time consuming and energy efficient, has been used for the fabrication of organic nanoparticles (**ONPs**). The rapid mixing of hydrophobic organic probe, **1**, and large volume of water changed the microenvironment of **1** and consequent precipitation of **1** led to formation of stable dispersion of nanoparticles in aqueous medium [21,22].

Due to the unavoidable effects of various physical parameters such as nature of organic solvent, concentration of organic compound, temperature and sonication time on formation and stability of **ONPs**, optimization of these parameters was conducted. Amongst various tested organic solvents (CH₃CN, CHCl₃, DMF, DMSO and THF), DMSO was found to be the most suitable for formations of **1-ONPs** with smallest nanoparticle size of 82.09 nm and least polydispersity index value of 0.180, as measured using DLS (Table 1).

Concentration of organic probe also plays significant role in the synthesis of organic nanoparticles, so, different concentrations of organic compound **1** (0.25 mM, 0.5 mM, 1 mM and 2 mM) have been used for fabricating **1-ONPs** in DMSO as the optimized organic solvent. As can be seen from Fig. S1a, the results supported 1 mM concentration of **1** as the optimum concentration for nanoparticles fabrication. As the nucleation process involved in nanoparticles formation is dependent on temperature, therefore, synthesis of **1-ONPs** was carried out at different temperatures. The studies revealed that the nanoaggregates developed were of appropriate size range at the temperature equal to or less than 10 °C (Fig. S1a). The size of **ONPs** started increasing with increase in the temperature of the solution. Size of the resultant **ONPs** was also dependent on the ratio of DMSO to water, where it was observed that increasing amount of DMSO led to the formation of large size particles due to aggregation (Fig. S1b). The effect of pH on the organic nanoparticle formation was recorded and as it is clear from Table S1, the best pH value for the synthesis of organic nanoparticles of required size range is 6.86, which is the pH of pure deionized water (D.I.) taken during the experiment.

3.2. DLS and TEM analysis of fabricated **1-ONPs**

The formation and stability of **1-ONPs** was monitored by DLS and



Scheme 1. Synthesis of compound **1** using solvent free approach.

Table 1

Particle size and polydispersity index value of fabricated **1-ONPs** in various solvents.

Solvent	Particle size (in nm)	Polydispersity Index (PDI)
CH ₃ CN	229.3	0.481
CHCl ₃	356.2	0.708
DMF	307.6	0.721
DMSO	82.09	0.180
THF	147.7	0.874

TEM techniques. Under optimized conditions, the DLS experiment showed that the particles have size of 42.84 nm. The DLS study provides hydrodynamic diameter of the particles due to the presence of solvent shell around the nanoparticles and therefore lacks the actual size determination. Therefore, to find the nearest obtainable size of nanoparticles, TEM analysis was performed. The particles size was approximately ~16 nm, obtained from the size intensity curve provided in the inset in Fig. 1b. This difference in the sizes from both the studies could be attributed to the difference in defining principle of both the techniques. To ensure the reproducibility of the 1-ONPs, the procedure was repeated four times and the obtained results approved the synthetic procedure.

3.3. Fluorescence recognition studies with organic nanoparticles (1-ONPs)

The emission spectra of organic probe **1** and 1-ONPs were analysed in order to see the spectral difference between organic compound **1** and its organic nanoparticles. The fluorescence emission peak underwent significant changes with reduced intensity, red shift and broadening of the emission peaks (Fig. S2). These changes are in agreement with the supra-molecular self-organization and intermolecular π - π interactions typically observed in organic nanoparticles [23].

The metal ion binding ability of synthesized 1-ONPs was determined by fluorescence emission spectroscopy in the absence and presence of various metal ions such as Na^+ , K^+ , Mg^{2+} , Al^{3+} , Mn^{2+} , Fe^{2+} , Fe^{3+} , Co^{2+} , Ni^{2+} , Cu^{2+} , Zn^{2+} , Cd^{2+} , Hg^{2+} and Pb^{2+} (added as their perchlorate salts). When excited at 280 nm wavelength, the organic nanoparticles displayed emission maxima at 406 nm with an observable stoke's shift of 126 nm ($\Phi_S = 0.14$). Upon addition of 100 equivalents of each of the above-mentioned ions, the fluorescence spectra of 1-ONPs underwent perturbations with addition of only Fe^{3+} ions (Fig. 2a). This feature revealed that 1-ONPs can serve as selective fluorescent nano-chemosensor for Fe^{3+} ions in an aqueous system.

Fluorescence titration analysis was performed in order to study the binding ability of 1-ONPs with Fe^{3+} ions. The fluorescence emission intensity was measured for each subsequent addition of Fe^{3+} ions to 1-ONPs and it was observed that peak intensity decreased with increasing concentration of Fe^{3+} ions (0–88.8 equiv) in 1-ONPs (Fig. 2b). Fe^{3+} is a well known paramagnetic ion with an empty d shell and has the ability to quench the fluorescence of a fluorophore via a photoinduced metal-to-fluorophore electron or energy transfer mechanism [24]. Moreover, Fe^{3+} has high thermodynamic affinity for ligands with "N" or "O" atoms leading to formation of stable complex. So, large fluorescence quenching was observed at 406 nm upon addition of Fe^{3+} ions to aqueous solution

of 1-ONPs. The designed nano-chemosensor displayed linear responses in two different ranges of Fe^{3+} ion concentration. The low concentration plot ranges from 0 to 33.3 equiv and the high concentration plot ranges from 33.3 to 88.8 equiv of Fe^{3+} ions (Fig. S3a). The limit of detection (LOD) value of 16.99 μM for Fe^{3+} detection was calculated using equation $\text{LOD} = 3\sigma/s$, where, σ is standard deviation and s is the slope of the calibration curve between fluorescence intensity and concentration of Fe^{3+} ions. The binding ability of 1-ONPs with the Fe^{3+} was determined with the help Benesi Hildebrand plot (Fig. S3b) and the association constant value which is equal to intercept/slope was obtained as $3.3 \times 10^3 \text{ M}^{-1}$. The equation employed is as follows [25]

$$\frac{1}{I - I_0} = \frac{1}{I_{\max} - I_0} + \frac{1}{(I_{\max} - I_0)K_a[Q]}$$

where I is the observed fluorescence intensity, I_0 is the fluorescence intensity of 1-ONPs in the absence of Fe^{3+} ions and I_{\max} is the intensity of 1-ONPs in the presence of excess Fe^{3+} ions. $[Q]$ represents the concentration of quencher, here it is Fe^{3+} ions and K_a represents association constant.

To investigate further the practical applicability of 1-ONPs as Fe^{3+} selective fluorescent sensor, competitive experiments were performed in the presence of various metal ions. To carry out this experiment, 100 equiv. of all interfering metal ions were introduced into the mixture containing 10 μM of 1-ONPs solution and 100 equivalents of Fe^{3+} ions. As is clear from fig S4, the quenching of 1-ONPs is almost identical to that observed in the presence of Fe^{3+} ions alone, pointing to the fact that fabricated 1-ONPs could serve as potential candidate as selective Fe^{3+} ion sensor in practical environmental applications.

3.4. Electrochemical analysis

The electrochemical response has been explored by recording cyclic voltammograms (CV) of chemosensor **1** and 1-ONPs within wide potential window of -2.0 V to $+2.0 \text{ V}$ at a scan rate of 50 mV/s. CV of chemosensor **1** (Fig. S5) with concentration of 10^{-5} M is displaying dismayed oxidation-reduction peaks while it is clearly observable that conversion of chemosensor **1** (bulk supramolecule) to ONPs has resulted in the emergence of new redox peaks along with amplified current response. In 1-ONPs (Fig. S5.), the new anodic peaks are seen at $+0.62 \text{ V}$ and $+1.13 \text{ V}$ along with a weak anodic hump at $+0.13 \text{ V}$. In addition to this shift in cathodic peaks was also observed. The amplified current response is accredited to the increased charge transfer rate and additional active sites generated due to enhanced surface to volume ratio after conversion of chemosensor **1** to ONPs [26].

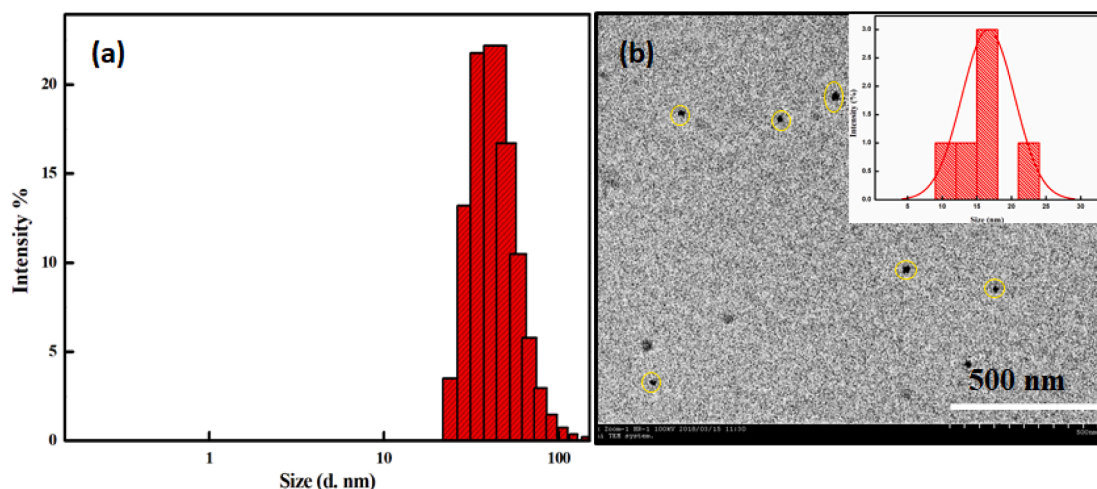


Fig. 1. (a) DLS graph of fabricated 1-ONPs and (b) TEM images of fabricated 1-ONPs with intensity curve showing average size of 16 nm.

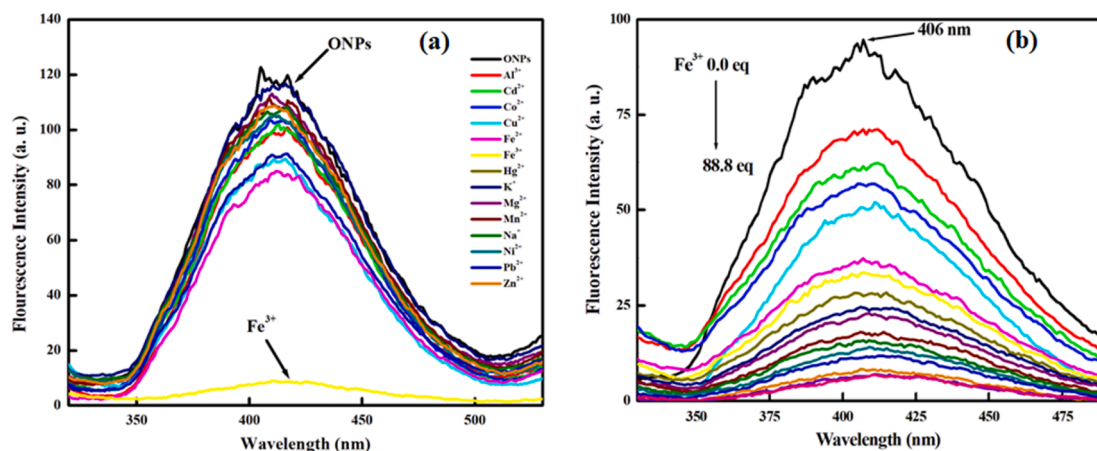


Fig. 2. Fluorescence spectra of 1-ONPs (a) in the presence of 100 equivalents of different metal ions and (b) with different concentrations of Fe^{3+} ions in aqueous medium.

3.5. Electrochemical recognition studies with organic nanoparticles (1-ONPs)

The electro-analytical response of 1-ONPs in presence of different metal ions (Al^{3+} , Cd^{2+} , Co^{2+} , Cu^{2+} , Fe^{2+} , Fe^{3+} , Hg^{2+} , K^+ , Mg^{2+} , Mn^{2+} , Na^+ , Ni^{2+} , Pb^{2+} and Zn^{2+}) was monitored to check for the selectivity (Fig. 3). For the recognition experiments, square wave anodic stripping voltammetry (SWASV) was carried out between the potential range of -1.5 V to $+1.0$ V using 1-ONPs (concentration used during experiments is 10^{-5} M) to which 100 equivalents of metal ions were added. After adding the 100 equivalents of each metal ion to ONPs solution, the mixture was left undisturbed to ensure complete binding. It is clearly evident from Fig. 3a, that maximum change in amperometric current response was observed in Fe^{3+} ion and hence further optimization was carried out to obtain high sensitivity for the developed method. Usually, benzothiazole moieties offered either formation of new complex or undergo protonation behavior. The anodic peaks in SWASV of Fig. 3b showed the appearance of new peaks (at -0.967 V and -0.683 V) pointing to the formation of stable complex due to high thermodynamic affinity of Fe^{3+} for ligands with “N” or “O” atoms.

3.5.1. Optimization of stripping analysis parameters:

To obtain maximum sensitivity of ONPs towards Fe^{3+} , optimization of deposition potential and deposition time was carried out. For this, deposition potential was varied from -0.9 V to -0.1 V where maximum anodic stripping current response was obtained at -0.8 V and thus

utilized for further studies. At a fixed deposition potential of -0.8 V, deposition time was also varied from 20 s to 60 s, where a maximum in stripping peak arises at 45 s. Thus, the optimized deposition potential of -0.8 V and deposition time of 45 s was approved for further studies. (Fig. S6).

3.5.2. Analytical performance of ONPs towards Fe^{3+} metal ions:

To check the legitimacy of the proposed SWASV method for the determination of Fe^{3+} ions, the stripping peak current response was monitored at different concentrations of Fe^{3+} ions (Fig. 4). The gradual increase in peak current was seen with increasing concentration of Fe^{3+} ions (from 0.3 μM to 8 μM). Also, a set of linear ranges from 0.3 μM to 0.95 μM and 1.0 μM to 8 μM were observed with limit of detection of 5.67×10^{-8} M and 5.17×10^{-7} M respectively.

The improved limit of detection of 1-ONPs using electrochemical mode rather than fluorescence here indicated its pre-eminence for the detection of Fe^{3+} ions. The calculated limit of detection value is comparable with the previously reported values (Table S2).

3.5.3. Interference studies

To monitor the effects of interferents, equal amounts of Fe^{3+} and different metal ions (Al^{3+} , Cd^{2+} , Co^{2+} , Cu^{2+} , Fe^{2+} , Fe^{3+} , Hg^{2+} , K^+ , Mg^{2+} , Mn^{2+} , Na^+ , Ni^{2+} , Pb^{2+} and Zn^{2+}) were administered to 10 ml of ONPs (10^{-5} M) solution. Fig. S7 indicates the least variation in stripping current response of Fe^{3+} ions in presence of these metal ions. Further, the analysis of interference was done using the equation:

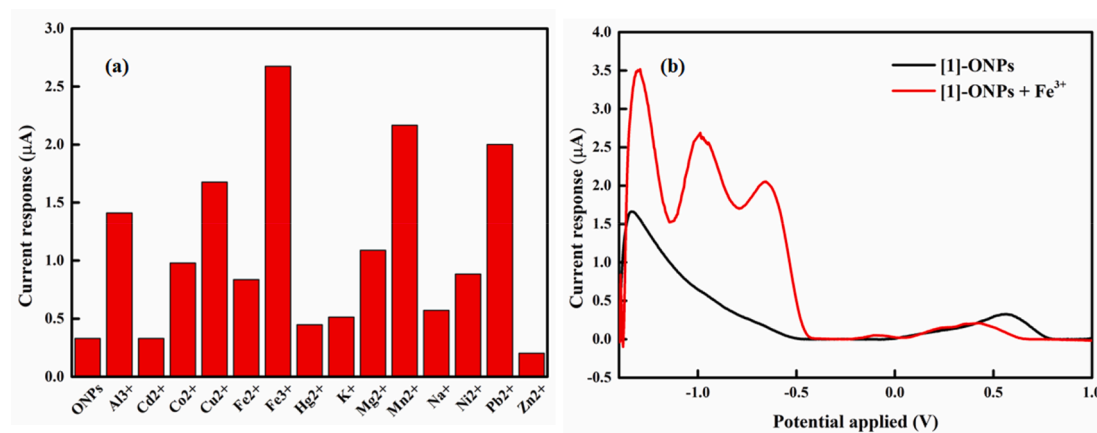


Fig. 3. (a) Bar graphs depicting the change in stripping current response of 1-ONPs (10^{-5} M) after addition of 100 equivalent of different metal ions and (b) Square wave stripping response of 1-ONPs (10^{-5} M) after addition of 100 equivalent of Fe^{3+} ions.

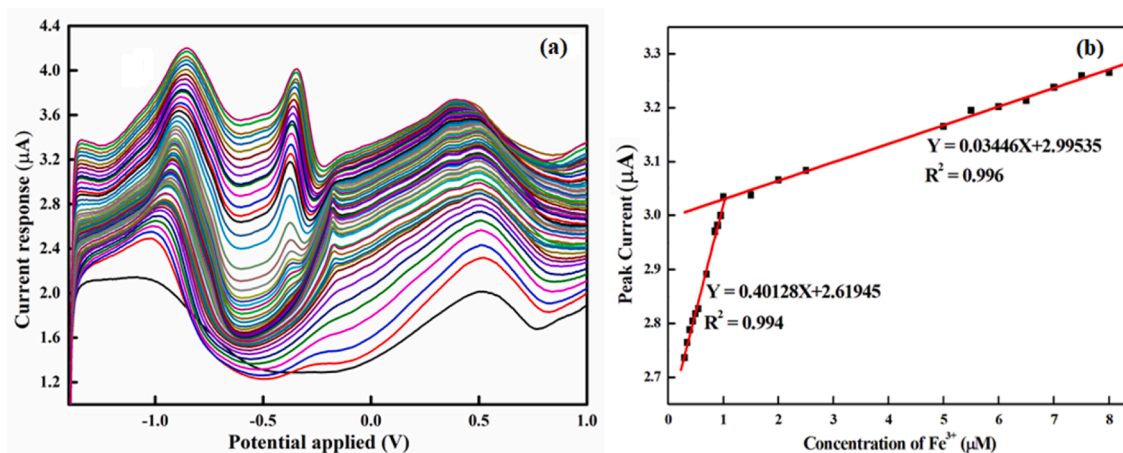


Fig. 4. (a) Titrimetric analysis of ONPs in the presence of Fe^{3+} from 0.3 μM to 8 μM and (b) Calibration plot between current response and Fe^{3+} concentration in organic nanoparticles solution.

$$\text{Interference}(\%) = (I_0 - I)/I_0 \times 100$$

where, I_0 refers to the peak current for Fe^{3+} ion and I refers to the peak current for Fe^{3+} and the interferents (Other metal ions) [27]. There is no significant interference from any of these metal ions except Pb^{2+} (7.90%) that hints the applicability of the proposed sensor to real time analysis.

3.5.4. Real time monitoring:

The designed **1-ONPs** were examined for its reliability for Fe^{3+} sensing in iron tablets. For this, different solutions of iron tablets were analysed by using Fluorescence spectroscopy and SWASV. The response obtained was noted down and compared with the calibration curves obtained with different concentrations of Fe^{3+} to calculate the amount of Fe^{3+} present in the prepared samples. The expected amount of iron in prepared samples was in close agreement with that of amount found as shown in Tables 2 and 3. The appreciably high recovery (%) of 90 to 103.7% indicated the applicability of prepared ONPs for real time monitoring.

Table 2

Real sample analysis of Fe^{3+} in iron tablets and their recovery (%) using Fluorometric analysis.

Iron tablet	Expected (M)	Found (M)	Recovery (%)	RSD (%)
Sample 1	32×10^{-5}	30.12×10^{-5}	94.1	1.09
Sample 2	48×10^{-5}	43.13×10^{-5}	90.0	2.13
Sample 3	64×10^{-5}	58.75×10^{-5}	91.8	3.46

Table 3

Real time analysis of Fe^{3+} in iron tablets and their recovery (%) using SWASV.

Iron tablet	Expected (μM)	Found (μM)	Recovery (%)	RSD (%)
Sample 1	0.4	0.39	97.5	1.2
Sample 2	0.6	0.55	91.0	3.1
Sample 3	0.8	0.83	103.7	1.4

4. Conclusions

New selective and sensitive nano sensor has been developed for the fluorescent as well as redox sensing of Fe^{3+} ions in aqueous solution using benzothiazole based organic nanoparticles (**1-ONPs**). The nano-precipitation method was used for the preparation of nanoparticles and **1-ONPs** were well characterized by DLS and TEM techniques. The nanoparticles exhibited “on-off” type fluorescent changes with high selectivity in the presence of Fe^{3+} ions, most probably due to its paramagnetic nature as well as its high affinity towards ligands with “N” or “O” atoms. An enhanced current response due to high surface to volume ratio facilitated by the increase in the number of active sites on conversion to ONPs has resulted in better sensitivity for Fe^{3+} in comparison to optical mode. Besides these, the designed **1-ONPs** were also examined for their real time application for Fe^{3+} sensing in iron tablets accentuating on their expediency.

CRedit authorship contribution statement

Navneet Kaur: Conceptualization, Resources. **Randeep Kaur:** Methodology, Visualization, Investigation, Data curation, Writing - original draft. **Ranjeet Kaur:** Investigation, Data curation. **Shweta Rana:** Supervision, Conceptualization, Resources, Funding acquisition.

Declaration of Competing Interest

The authors declare that they have no known competing financial interests or personal relationships that could have appeared to influence the work reported in this paper.

Acknowledgements

Financial grant from Department of Science and Technology-Science and Engineering Research Board (Grant No. SERB/2016/000046) is gratefully acknowledged by the authors.

Appendix A. Supplementary data

Supplementary data to this article can be found online at <https://doi.org/10.1016/j.inoche.2021.108648>.

References

- [1] V.P. Sharma, U. Sharma, M. Chattopadhyay, V.N. Shukla, Advance applications of nanomaterials: a review, *Mater. Today* 5 (2018) 6376.
- [2] O.V. Salata, Applications of nanoparticles in biology and medicine, *J. Nanobiotechnol.* 2 (2004) 3.
- [3] F. Valentini, G. Palleschi, Nanomaterials and analytical chemistry, *Anal. Lett.* 41 (2008) 479.
- [4] W. Wu, Inorganic nanomaterials for printed electronics: a review, *Nanoscale* 9 (2017) 7342.
- [5] A. Munawar, Y. Ong, R. Schirhagl, M.A. Tahir, W.S. Khan, S.Z. Bajwa, Nanosensors for diagnosis with optical, electric and mechanical transducers, *RSC Adv.* 9 (2019) 6793.
- [6] I. Khan, K. Saeed, I. Khan, Nanoparticles: properties, applications and toxicities, *Arab. J. Chem.* 12 (2019) 908.
- [7] F. Debuigne, L. Jeunieau, M. Wiame, J.B. Nagy, Synthesis of organic nanoparticles in different w/o microemulsions, *Langmuir* 16 (2000) 7605.
- [8] A. Saini, A.K.K. Bhasin, N. Singh, N. Kaur, Development of a Cr(III) ion selective fluorescence probe using organic nanoparticles and its real time applicability, *New J. Chem.* 40 (2016) 278.
- [9] J. Mishra, M. Kaur, N. Kaur, A.K. Ganguli, Highly selective and sensitive simultaneous nanomolar detection of Cs(I) and Al(III) ions using tripodal organic nanoparticles in aqueous media: the effect of the urea backbone on chemosensing, *RSC Adv.* 10 (2020) 22691.
- [10] R. Kaur, S. Saini, N. Kaur, N. Singh, D.O. Jang, Rhodamine-based fluorescent probe for sequential detection of Al^{3+} ions and adenosine monophosphate in water, *Spectrochim. Acta A: Molecul. Biomol. Spectroscop.* 225 (2020) 117523.
- [11] P.G. Mahajan, J.S. Shin, N.C. Dige, B.D. Vanjare, Y. Han, Chelation enhanced fluorescence of rhodamine based novel organic nanoparticles for selective detection of mercury ions in aqueous medium and intracellular cell imaging, *J. Photochem. Photobiol. A* 397 (2020) 112579.
- [12] B.K. Billing, J. Singh, P.K. Agnihotri, N. Singh, Development of electrochemical sensor for selective recognition of PO_4^{3-} ions using organic nanoparticles of dipodal receptor in aqueous medium, *Electrochim. Acta* 182 (2015) 1112.
- [13] S. Kumar, S.K. Mittal, N. Kaur, Enhanced performance of organic nanoparticles of a Schiff-base for voltammetric sensor of Cu(II) ions in aqueous samples, *Anal. Methods* 11 (2019) 359.
- [14] R. Kaur, G. Dhaka, P. Singh, S. Rana, N. Kaur, Optical and electrochemical recognition studies of anions via novel benzothiazole azo-derivative, *Arab. J. Chem.* 13 (2020) 6931.
- [15] C.A. Rusinek, A. Bange, M. Warren, W. Kang, K. Nahan, I. Papautsky, W. R. Heineman, Bare and polymer-coated indium tin oxide as working electrodes for manganese cathodic stripping voltammetry, *Anal. Chem.* 88 (2016) 4221.
- [16] R. Kaur, S. Rana, R. Singh, V. Kaur, P. Narula, A Schiff base modified graphene oxide film for anodic stripping voltammetric determination of arsenite, *Microchim. Acta* 186 (2019) 741.
- [17] N. Abbaspour, R. Hurrell, R. Kelishadi, Review on iron and its importance for human health, *J. Res. Med. Sci.* 18 (2014) 164.
- [18] Y. Dong, H. Zhang, F. Lei, M. Liang, X. Qian, P. Shen, H. Xu, Z. Chen, J. Gao, J. Yao, Benzimidazole-functionalized Zr-Uio-66 nanocrystals for luminescent sensing of Fe^{3+} in water, *J. Solid State Chem.* 245 (2017) 160.
- [19] H. Xu, J. Gao, X. Qian, J. Wang, H. He, Y. Cui, Y. Yang, Z. Wang, G. Qian, Metal-organic framework nanosheets for fast-response and highly sensitive luminescent sensing of Fe^{3+} , *J. Mater. Chem. A* 4 (2016) 10900.
- [20] B.K. An, S.K. Kwon, S.D. Jung, S.Y. Park, Enhanced emission and its switching in fluorescent organic nanoparticles, *J. Am. Chem. Soc.* 124 (2002) 14410.
- [21] K. Ujiye-Ishii, E. Kwon, H. Kasai, H. Nakanishi, H. Oikawa, Methodological features of the emulsion and reprecipitation methods for organic nanocrystal fabrication, *Cryst. Growth Des.* 8 (2008) 369.
- [22] H. Jiang, X. Sun, M. Huang, Y. Wang, D. Li, S. Dong, Rapid self-assembly of Oligo (ophenylenediamine) into one-dimensional structures through a facile reprecipitation route, *Langmuir* 22 (2006) 3358.
- [23] C.A. Huerta-Aguilar, P. Raj, P. Thangarasu, N. Singh, Fluorescent organic nanoparticles (FONs) for selective recognition of Al^{3+} : application to bioimaging for bacterial sample, *RSC Adv.* 6 (2016) 37944.
- [24] R. Azadbakht, M. Hakimi, J. Khanabadi, Fluorescent organic nanoparticles with enhanced fluorescence by self-aggregation and their application for detection of Fe^{3+} ions, *New J. Chem.* 42 (2018) 5929.
- [25] H.A. Benesi, J.H. Hildebrand, A spectrophotometric investigation of the interaction of iodine with aromatic hydrocarbons, *J. Am. Chem. Soc.* 71 (1949) 2703.
- [26] A. Gessner, A. Lieske, B.R. Paulke, R.H. Müller, Influence of surface charge density on protein adsorption on polymeric nanoparticles: analysis by two-dimensional electrophoresis, *Eur. J. Pharm. Biopharm.* 54 (2002) 165.
- [27] G. Dhaka, G. Jindal, R. Kaur, S. Rana, A. Gupta, N. Kaur, Multianalyte azo dye as an on-site assay kit for colorimetric detection of Hg^{2+} ions and electrochemical sensing of Zn^{2+} ions, *Spectrochim. Acta A: Mol. Biomol. Spectr.* 229 (2020) 117869.